GEOELECTRICAL INVESTIGATION OF THE SUBSURFACE LITHOLOGY AT THE PROPOSED INTERNATIONAL STADIUM, MINNA, NIGER STATE, NIGERIA

Supported by tetfund

Jamiu Alani Sikiru, Adetona Adebayo Abbass, Jamilu Shehu* and Aisha Alkali
Department of Geophysics, Federal University of Technology, Minna, Nigeria
*Corresponding author: jameelshehu@futminna.edu.ng

Received: January 20, 2020 **Accepted:** May 12, 2020

Abstract: Geoelectrical investigation was carried out to evaluate the viability and to determine the subsurface Lithology, depth to bedrocks as well as to establish prolific aquifers at the proposed Minna International Stadium, Niger State, Nigeria. The area is located at the Basement Complex of Nigeria which comprises of: Migmatites-Gneiss Complex, the Schist Belt, the older granites and undeformed acidic/basic dykes. Vertical electrical sounding (VES) surveys were conducted using a resistivity meter along six (6) profiles, at 50 m interval from each sounding point; and a total of 36 VES measurement were made. The results of the VES suggests that the entire subsurface of the proposed stadium, is made up of three (3) distinctive Lithologies; the First layer is Top Soil/Lateritic Particles with resistivity value between 20.38 and 272.8 Ωm it thickness is between 0.09 m to 5.84 m, the Second layer is a weathered/fractured basement with resistivity values variation between 45.15 and 1017 Ωm, its thicknesses ranges between 2.54 m and 24.9 m and the Third layer is fresh basement with resistivity values from 1259 to 3606 Ωm. The result of this work shows that the second layer is generally weathered Basement, it is therefore advisable for engineers to consider this in their design. The foundations should be situated towards the southeastern, southwestern and northern section of the site, where the bedrocks are shallow, uplifted and consolidated. The site is suitable and viable for the construction of the proposed stadium; the depth to bedrocks is more than 2.54 m from the surface. Borehole should be drilled on the following VES points; A6, B3, B4, C6, C1, C2, D1, D3, E2, E3, F2 and F1, these VES points depicts zones of good fractures.

Keywords: Stadium, lithology, consolidated, subsurface, geoelectrical

Introduction

The use of geophysical methods to indirectly investigate construction sites in many parts of the world is now popularly accepted by scientists, engineers and investors Aderoju and Adebayo (2015). Geophysical site investigation minimizes the cost of direct boring/drilling into the subsurface and it has a wide coverage of various materials occurring at a particular site, (Bell 2007). Over the years many stadiums have been reported collapsed, for instance, parts of Maracana Stadium, Brazil, Collapsed in 2013, Metrodome Stadium U S A failed in 2010, in Brussels, Belgium the Heysel Stadium Disaster occurred in 1985, Stadiums failure were reported at Dallas, Washington, Malaysia, Iran and China (Ranker, 2017). Geoelectrical investigation was carried out to determine the subsurface Lithology, depth to consolidated rocks as well as to establish prolific aquifers within Proposed International Stadium, Minna, Nigeria.

Both active and passive geophysical methods are used in assessing engineering construction site to ascertain the site's viability for any proposed infrastructure. Most Stadiums failed due to poor planning, for instance Bako Kontagora Stadium, Minna and Tangshan Stadium, Heibe Province, China failed since its pitch was not on a consolidated ground (Qing-Ke *et al.,* 2014). To eradicate such problem, proper geophysical survey need to be carried out to delineate the Lithology in order to ascertain the depth to consolidation level.

At the moment all over the world, there are numerous cases of stadium collapsed and roof failure due to both poor foundation and lack of proper site investigations as well as improper designs that consequently subjects these giant structures to preventable hazards. The need to search for site where the bedrock is consolidated and very shallow which can provide strong base for such giant infrastructures like Stadiums is very important.

Stadium construction is capital intensive, it cost between \$100 to \$350 Million and more in some cases. Geophysical investigation provide relevant picture about the geology and the subsurface Lithology existing beneath any proposed site.

Materials and Methods

Geology of the area

Minna is surrounded by rugged terrain of granitic rocks at north-eastern section, the rocks in Minna environs are mainly meta-sedimentary and meta-igneous in nature, and they have undergone many phase deformation and metamorphism. The Pan-African age intrusive rock cross cut the basement rocks, these intrusions forms the Minna and Paiko famous and pronounced Batholiths.

Generally, five lithologic units can be recognized, these includes the schist occurring as a low-lying unit around southwest-north portion of the central part of Minna City, the Gneiss form suites at the Northern and Southern part making an observable contact with the granite deposit. Felspathic-Pegmatite is found at the eastern part. Minna area generally has thin overburden ranging from 3-7 metres (Alabi, 2011).

Residents and estate developers take advantage of this thin overburden during excavation for foundation. Minna is the capital city of Niger State, North Central Nigeria; the International Stadium is to be located along Minna-Zungeru road at a proposed site around a Settlement called *RafinYashi* before Nigeria Air Force (NAF) Base, along Airport road, *Maikunkele*, Minna (Fig. 1).

The stadium lies at 9°40'23.70''N to 9°40'27.27''N and 6°29'52.30'' E to 6°29'54.74'' E. The proposed stadiums' land is 05-10 hectares directly by Airport road. The land is relatively rocky and undulating in some areas. Minna is generally under lied by basement complex rocks, mostly Pre-Cambrian igneous and metamorphic rocks outcropping at some places.

The Minna Batholith is a major feature trending from Northern to Eastern part of the city, this limits urban development in that direction. Minna City lied on 6,784 square kilometers and has about 500,000.00 populations (National Population Commission 2006). The city has a mean annual rainfall of 1300 mm; the highest mean monthly rainfall is in September with about 3000 mm. On the average the raining season starts between April and ends October in a year. The temperature often ranges between 22°C to 40°C in some months.

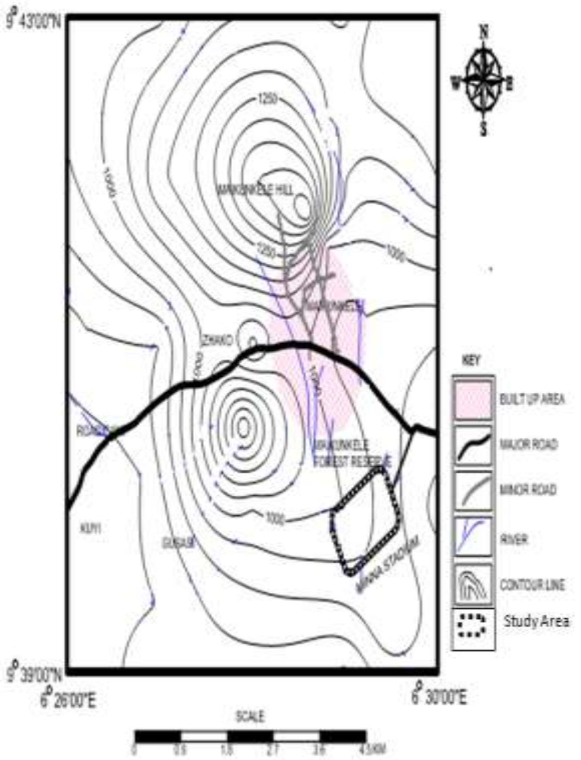

Fig. 1: Location map of international stadium

Methods

An electrical resistivity survey involves laying out a series of electrodes, each driven into the ground about 50 cm (Fig. 2). Their spacing is depends on the depth of penetration required. The further apart the electrodes, the deeper the resistivity measurements of the subsurface that can be taken. Typically resistivity surveys range in depth from a few metres to more than 100 metres.

A total of Six (6) profiles with six (6) VES point along each profile of 250 m long (Fig. 3), was conducted. Readings were taken from 36 VES points 50 m apart. The instrument used was stationed at each VES point with a total number of six persons, two with current electrodes, two with potential electrodes and two with the system taken the readings. The study adapted a maximum of 100 m current electrode separation (AB/2) and maximum of 15 m potential (MN/2) electrode separation.

The readings were taken by increasing the current electrodes from 1 m to 100 m and potential electrodes spacing from 0.5 m to 15 m.

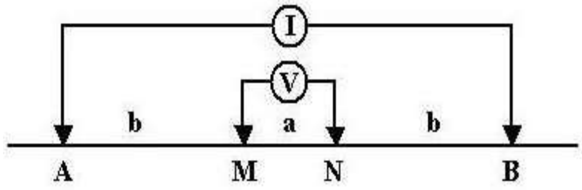

Fig. 2: Schlumberger electrode array

$$\rho = \pi \left[\frac{\left(\overline{AB}/2\right)^2 - \left(\overline{MN}/2\right)^2}{\overline{MN}} \right] \qquad (1)$$

Where: A=Current Electrode (+), B=Current Electrode (-), M=Potential Electrode, N=Potential Electrode, a=Distance between successive electrodes, $\overline{AB}$ =Distance between Current Electrodes, $\overline{MN}$ =Distance between Potential Electrodes and ρ this is the geometric factor, to be multiplied by resistivity reading to obtain apparent resistivity i.e. the resistivity contrast of various rocks.

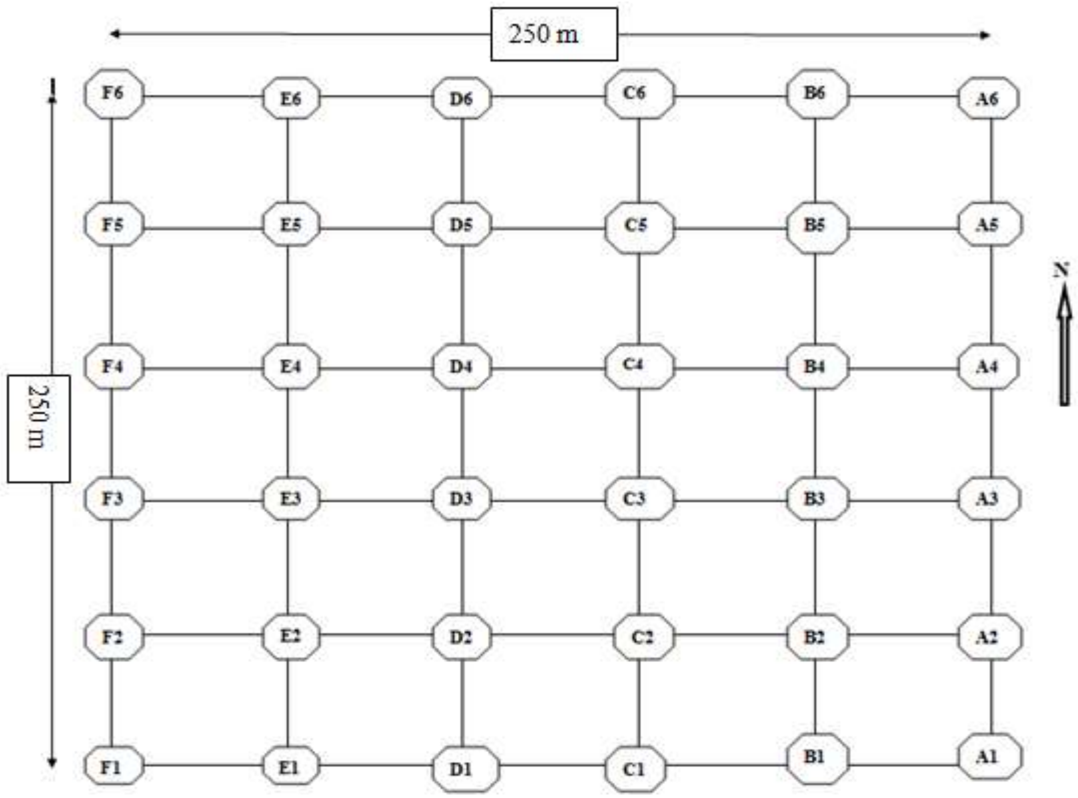

Fig. 3: Field profile layout

Results and Discussion

The data used for this research was acquired with a resistivity meter; it was in current (ampere) and voltage (volt) mode, the voltage was divided by the current to obtain the resistance (Ohm), in accordance to Ohm's law. The resistance (ohm) was then multiplied with the pre calculated geometric factor (equation 1) which gave us apparent resistivity (ohm-meter).

Apparent resistivity values for each Vertical Electrical Sounding (VES) points were plotted against current electrode separation (AB/2 m) using IPI2WIN inversion software (Alexey Bobachev, 2003). After inserting the values and a number of iteration, the software produced; the Geologic sections (delineating the different rock type with various distinctive colour), curves, with their corresponding number of layers, resistivity values, depth (m) and equivalent thickness (m) as well as percentage errors (Figs. 11 and 12, respectively).

Profile A

Table 1, Fig. 4a and b display the VES interpretation for profile A. Only VES A2 is a two layer models, the remaining VES A1 to A6 are three layer models. The profile shows A and H curve type. The following were deduced:

The first layer has resistivity values ranging from 20.38 to 66.89 Ωm. The highest resistivity value of 66.89 Ωm was obtained on VES A1, and the least resistivity value of 20.38 Ωm was found on VES A5. The profile is thickest at VES A2 (about 2.39 m) and thinnest at VES A6 (about 0.09 m).

The second layer's resistivity values ranges between 12.59 and 613 Ωm. Highest resistivity value is found at VES A2 (613 Ωm) and the smallest resistivity value of about 12.59 Ωm was found at VES A1. The layer is thickest at VES A6 (about 9.90 m) and thinnest at VES A1 (about 0.69 m).

The third layer has resistivity values ranging between 1259 Ωm and 3606Ωm. The highest resistivity value of 3606 Ωm is found at VES A4 and the lowest resistivity value of 1259 Ωm is found at VES A3. This layer is deepest at VES A6 and VES A4, shallowest at VES A1.

Table 1: Interpreted result of Profile A

VES Point	No. of Layers	Curve Type	Resistivity of Layers Ωm	Layer Thickness (m)	Depth of Layer (m)
A1	1		66.89	0.75	0.00
	2	H	12.59	0.69	0.75
	3		1953	∞	1.45
A2	1	A	31.01	2.39	0.00
	2		613	∞	2.39
A3	1	A	53.18	0.33	0.00
	2		66.07	5.17	0.33
	3		1259	∞	5.50
A4	1	A	25.5	0.16	0.00
	2		358	8.07	0.16
	3		3606	∞	8.23
A5	1	A	20.38	0.19	0.00
	2		355.8	4.90	0.19
	3		3169	∞	5.09
A6	1	A	27.01	0.09	0.00
	2		324.7	9.90	0.09
	3		1850	∞	9.99

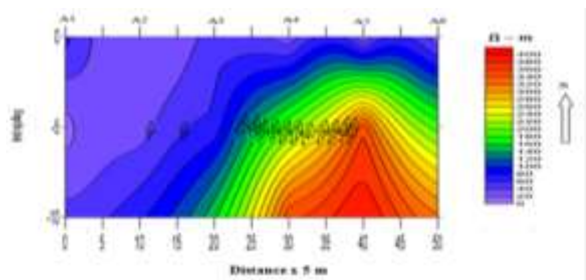

Fig. 4a: Vertical geoelectrical section of Profile A

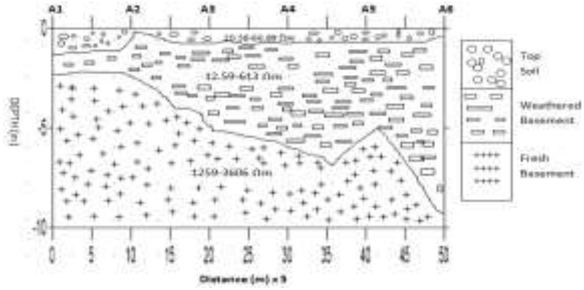

Fig. 4b: Geologic section of Profile A of the study area

Table 2: Interpreted result of Profile B

VES Point	No. of Layers	Curve Type	Resistivity of Layers Ωm	Layer Thickness (m)	Depth of Layer (m)
B1	1	H	181.3	0.54	0.00
	2		40.63	2.74	0.54
	3		1116	∞	3.29
B2	1	H	63.69	1.59	0.00
	2		33.15	2.98	1.59
	3		595.6	∞	4.57
B3	1	A	79	1.8	0.00
	2		516	24.9	1.8
	3		1696	∞	26.7
B4	1	A	37.75	1.43	0.00
	2		466.9	6.81	1.43
	3		1525	∞	8.23
B5	1	A	71.43	1.30	0.00
	2		322.2	6.32	1.30
	3		2696	∞	7.63
B6	1	A	43.5	1.35	0.00
	2		237.3	5.83	1.35
	3		2425	∞	7.18

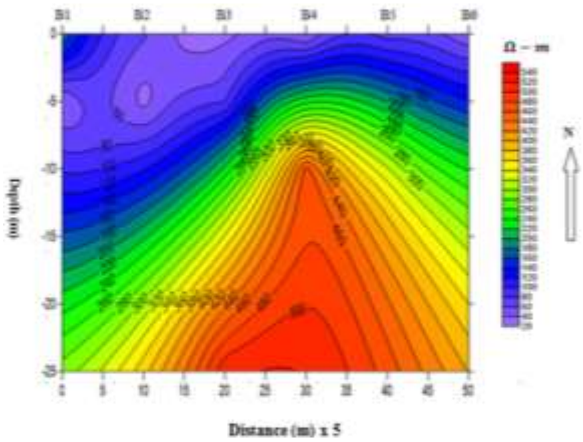

Fig. 5a: Vertical geoelectrical section of Profile B

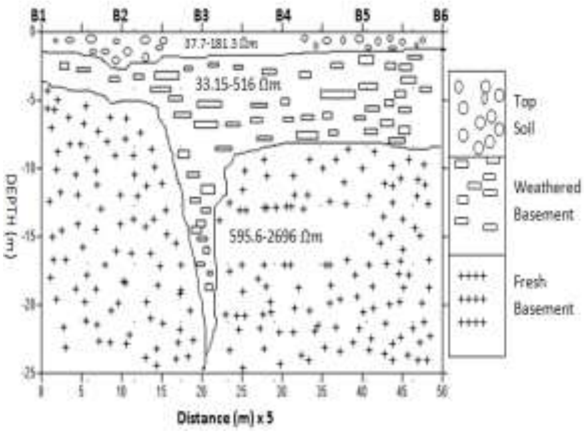

Fig. 5b: Geologic section of Profile B of the study area

Profile B

Table 2, Fig. 5a and b show the VES interpretation for profile B. VES B1 to B6 are three layer models. The profile shows A and H curve type. The following were deduced:

The first layer has resistivity values ranging from 37.7 to 181.3 Ωm. The highest resistivity value of 181.3Ωm was obtained on VES B1, and the least resistivity value of 37.7 Ωm was found on VES B4. The profile is thickest at VES B3 (about 1.8 m) and thinnest at VES B1 (about 0.54 m).

The second layer's resistivity values ranges between 33.15 to 516 Ωm. Highest resistivity value is found at VES B3 (516 Ωm) and the smallest resistivity value of about 33.15 Ωm was found at VES B2. The layer is thickest at VES B3 (about 24.9 m) and thinnest at VES B1 (about 2.74 m).

The third layer has resistivity values ranging between 595.6 to 2696 Ωm. The highest resistivity value of 2696 Ωm is found at VES B5 and the lowest resistivity value of 595.6Ωm is found at VES B2. This layer is deepest at VES B3 and VES B4, shallowest at VES B1.

Profile C

Table 3, Fig. 6a and b display the VES interpretation for profile C. VES C1 to C6 are three layer models. The profile shows A and H curve type. The following were deduced:

The first layer has resistivity values ranging from 27.91 to 86.79 Ωm. The highest resistivity value of 86.79 Ωm was obtained on VES C6, and the least resistivity value of 27.91 Ωm was found on VES C4. The layer is thickest at VES C1 (about 2.60 m) and thinnest at VES C5 (about 1.24 m).

The second layer's resistivity values ranges between 15.9 to 1017 Ωm. Highest resistivity value is found at VES C6 (1017 Ωm) and the smallest resistivity value of about 15.9 Ωm was found at VES C3. The layer is thickest at VES C6 (about 44.62 m) and thinnest at VES C5 (about 0.49 m).

The third layer has resistivity values ranging between 1425 to 30187 Ωm. The highest resistivity value of 3187 Ωm is found at VES C3 and the lowest resistivity value of 1425Ωm is found at VES C5. This layer is deepest at VES C6, C1 and VES C2, shallowest at VES C4.

Table 3: Interpreted result of Profile C

VES Point	No. of Layers	Curve Type	Resistivity of Layers Ωm	Layer Thickness (m)	Depth of Layers (m)
C1	1	A	35.8	2.60	0.00
	2		225.6	5.26	2.60
	3		1477	∞	7.86
C2	1	A	38.43	1.53	0.00
	2		129.2	6.23	1.53
	3		1503	∞	7.76
C3	1	H	66.91	2.11	0.00
	2		15.9	1.52	2.11
	3		30187	∞	3.63
C4	1	A	27.91	2.16	0.00
	2		667	0.49	2.16
	3		1173	∞	2.66
C5	1	A	82.3	1.24	0.00
	2		190.5	3.17	1.24
	3		1425	∞	4.40
C6	1	A	86.79	1.26	0.00
	2		1017	44.62	1.26
	3		3517	∞	45.88

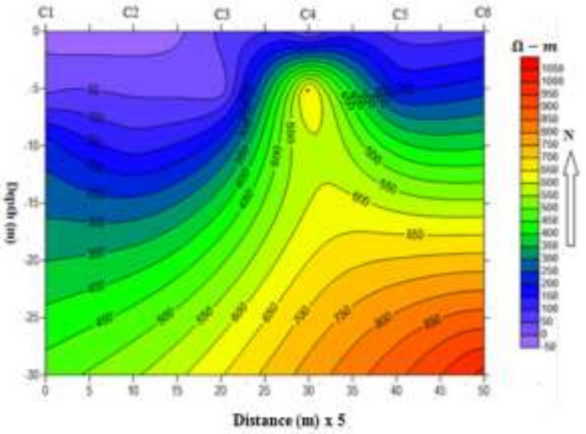

Fig. 6a: Vertical geoelectrical section of Profile C

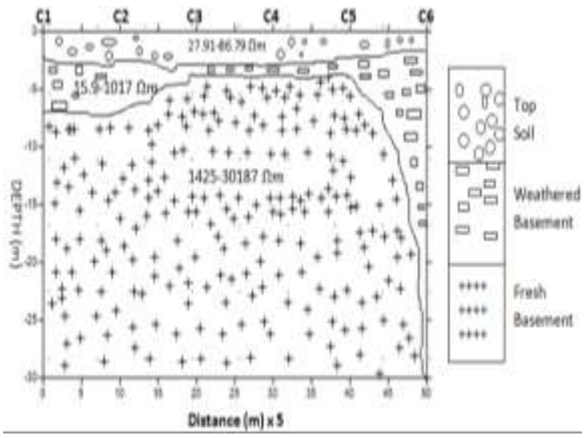

Fig. 6b: Geologic section of Profile C of the study area

Table 4: Interpreted result of Profile D

VES Point	No. of Layers	Curve Type	Resistivity of Layers Ωm	Layer Thickness (m)	Depth of Layer (m)
D1	1	A	33.94	1.24	0.00
	2		1045	8.88	1.24
	3		1704	∞	10.11
D2	1	A	22.19	1.13	0.00
	2		103.6	4.72	1.13
	3		2425	∞	5.85
D3	1	A	27.45	1.53	0.00
	2		124.2	7.70	1.53
	3		1173	∞	9.22
D4	1	H	107.9	3.49	0.00
	2		39.08	2.44	3.49
	3		1152	∞	5.94
D5	1	A	143	3.56	0.00
	2		108.3	4.41	3.56
	3		696.5	∞	7.97
D6	1	A	75.52	1.52	0.00
	2		269.6	5.48	1.52
	3		2794	∞	6.99

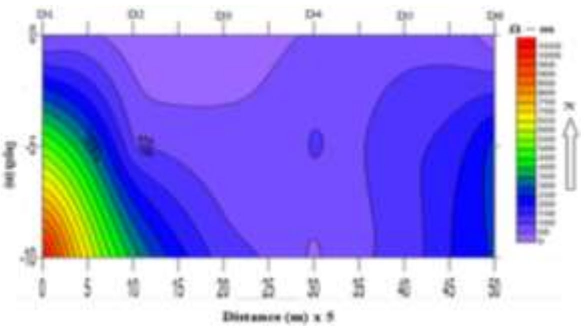

Fig. 7a: Vertical Geoelectrical Section of Profile D

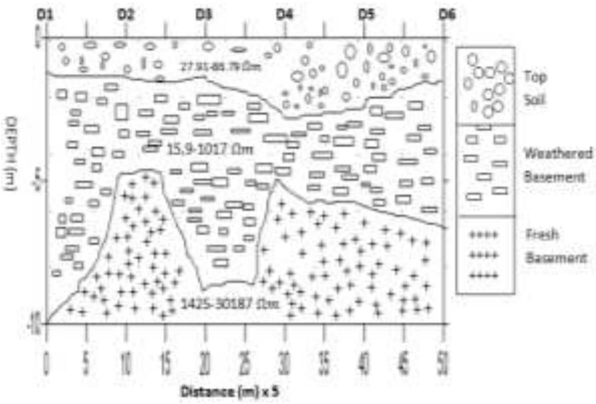

Fig. 7b: Geologic section of Profile D of the study area

Profile D

Table 4, Fig. 7a and b display the VES interpretation for profile D. VES D1 to D6 are three layer models. The profile shows A and H curve type. The following were deduced:

The first layer has resistivity values ranging from 22.19 to 143 Ωm. The highest resistivity value of 143 Ωm was obtained on VES D5, and the least resistivity value of 22.19 Ωm was found on VES D2. The layer is thickest at VES D5 (about 3.56 m) and thinnest at VES D2 (about 1.13 m).

The second layer's resistivity values ranges between 39.08 to 1045 Ωm. Highest resistivity value is found at VES D1 (1045 Ωm) and the smallest resistivity value of about 39.08 Ωm was found at VES D4. The layer is thickest at VES D1 (about 8.88 m) and thinnest at VES D4 (about 2.44 m).

The third layer has resistivity values ranging between 696.5 to 1704 Ωm. The highest resistivity value of 1704 Ωm is found at VES D1 and the lowest resistivity value of 696.5 Ωm is found at VES D5. This layer is deepest at VES D1, and VES D3, shallowest at VES D4.

Profile E

Table 5, Fig. 8a and b depicts the VES interpretation for profile E. VES E1 to E6 are three layer models. The profile shows A and H curve type. The following were deduced:

The first layer has resistivity values ranging from 41.25 to 272.8 Ωm. The highest resistivity value of 272.8 Ωm was obtained on VES E1, and the least resistivity value of 41.25 Ωm was found on VES E2. The layer is thickest at VES E3 (about 5.84 m) and thinnest at VES E5 (about 1.33 m).

The second layer's resistivity values ranges between 45.15 to 1566 Ωm. Highest resistivity value is found at VES E1 (1566 Ωm) and the smallest resistivity value of about 45.15 Ωm was found at VES E4. The layer is thickest at VES E2 (about 35.32 m) and thinnest at VES E6 (about 2.28 m).

The third layer has resistivity values ranging between 1132 to 3034 Ωm. The highest resistivity value of 3034 Ωm is found at VES E1 and the lowest resistivity value of 1132 Ωm is found at VES E3. This layer is deepest at VES E2, and VES E3, shallowest at VES E6.

Table 5: Interpreted result of Profile E

VES Point	No. of Layers	Curve Type	Resistivity of Layer Ωm	Layer Thickness (m)	Depth of Layer (m)
E1	1	A	272.8	1.38	0.00
	2		1566	5.40	1.38
	3		3034	∞	6.77
E2	1	A	41.25	1.59	0.00
	2		608.3	35.32	1.59
	3		1585	∞	36.91
E3	1	A	67.38	5.84	0.00
	2		150.3	5.30	5.84
	3		1132	∞	11.14
E4	1	H	177.9	1.39	0.00
	2		45.15	3.18	1.39
	3		1400	∞	4.57
E5	1	A	88.34	1.33	0.00
	2		150.3	7.15	1.33
	3		2219	∞	8.48
E6	1	H	210.4	3.49	0.00
	2		147.7	2.28	3.49
	3		1503	∞	5.77

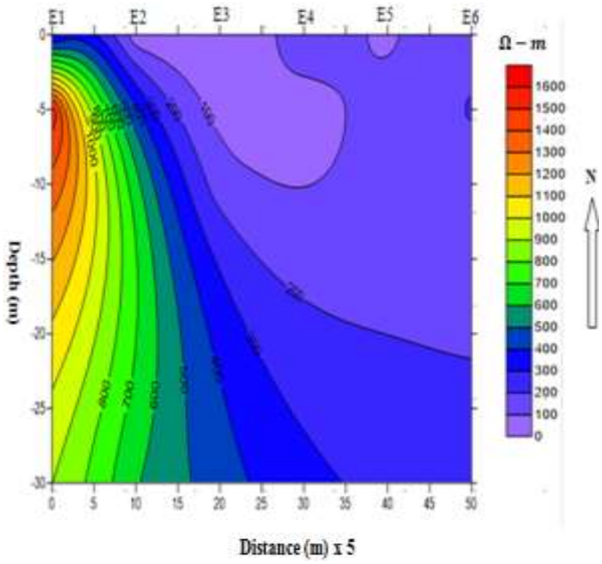

Fig. 8a: Vertical geoelectrical section of Profile E

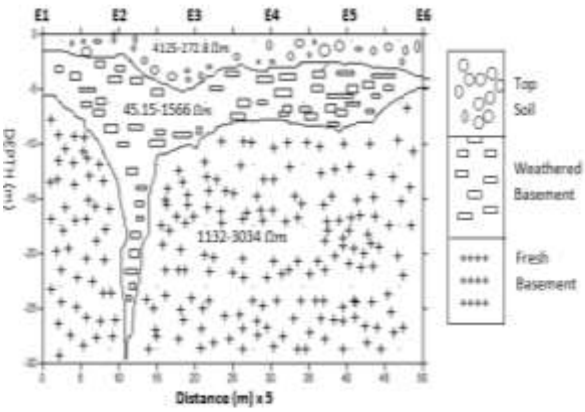

Fig. 8b: Geologic section of Profile E of the study area

Table 6: Interpreted result of Profile F

VES Point	No. of Layers	Curve Type	Resistivity of Layer Ωm	Thickness of Layer (m)	Depth of Layer (m)
F1	1	H	51.62	2.83	0.00
	2		43.76	17.97	2.83
	3		818.2	∞	20.79
F2	1	A	24.68	1.35	0.00
	2		338.8	36.89	1.35
	3		1732	∞	38.24
F3	1	A	24.24	4.55	0.00
	2		115.2	6.45	4.55
	3		1215	∞	11
F4	1	A	51.77	2.55	0.00
	2		167.1	5.83	2.55
	3		1859	∞	8.38
F5	1	H	108.8	1.92	0.00
	2		16.41	2.16	1.92
	3		867.9	∞	4.08
F6	1	A	32.76	1.34	0.00
	2		246.8	10.99	1.34
	3		2259	∞	12.36

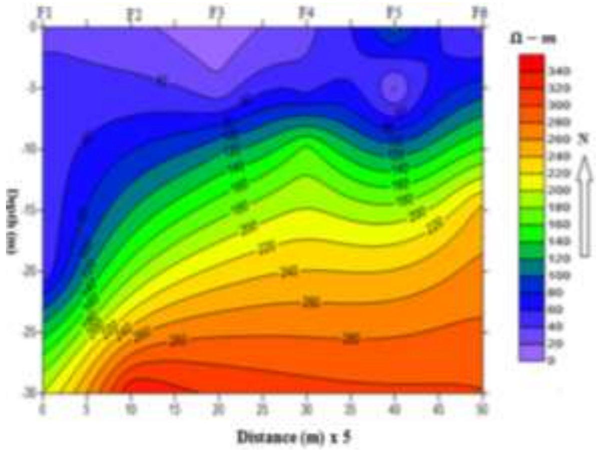

Fig. 9a: Vertical geoelectrical section of Profile F

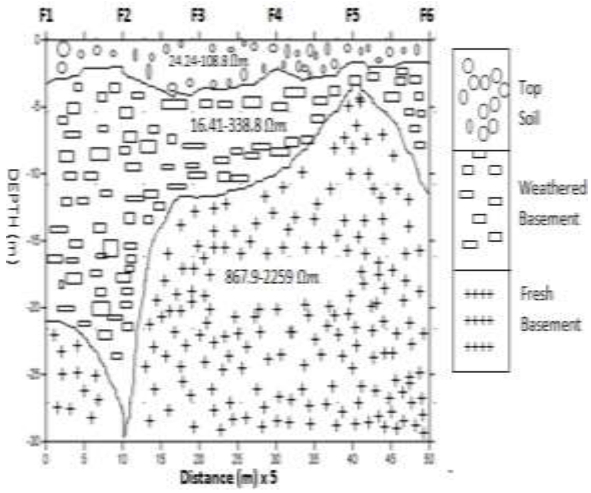

Fig. 9b: Geologic section of Profile F of the study area

Profile F

Table 6, Fig. 9a and b display the VES interpretation for profile F. VES F1 to F6 are three layer models. The profile shows A and H curve type. The following were deduced:

The first layer has resistivity values ranging from 24.24 to 108.8 Ωm. The highest resistivity value of 108.8 Ωm was obtained on VES F5, and the least resistivity value of 24.24 Ω□ was found on VES F3. The layer is thickest at VES F3 (about 4.55 m) and thinnest at VES F6 (about 1.34 m).

The second layer's resistivity values ranges between 16.41 to 338.8 Ωm. Highest resistivity value is found at VES F2 (338.8 Ωm) and the smallest resistivity value of about 16.41 Ωm was found at VES F5. The layer is thickest at VES F2 (about 36.89 m) and thinnest at VES F5 (about 2.16 m).

The third layer has resistivity values ranging between 867.9 to 2259 Ωm. The highest resistivity value of 2259 Ωm is found at VES F6 and the lowest resistivity value of 867.9 Ωm is found at VES F5. This layer is deepest at VES F2, and VES F1, shallowest at VES F5.

The depth to consolidation

The basement highs (areas with high resistivity values within the basement rocks as depicted by yellow and red colours in the iso resistivity map; (Fig. 10) indicates fresh basement which are important in foundation for the development of large infrastructure like the International Stadium. The basement lows (portions with low resistivity values) showed the weathered layer which is also consolidated and competent to serve as foundation base. As observed from the iso resistivity map, basement are pronounced at 10 m, while the basement rocks only outcrop at Northern and Southeastern portion of the study area within ≤5 m. Generally, the depth to consolidation within the study area ranges between 0.09 to 5.84 m.

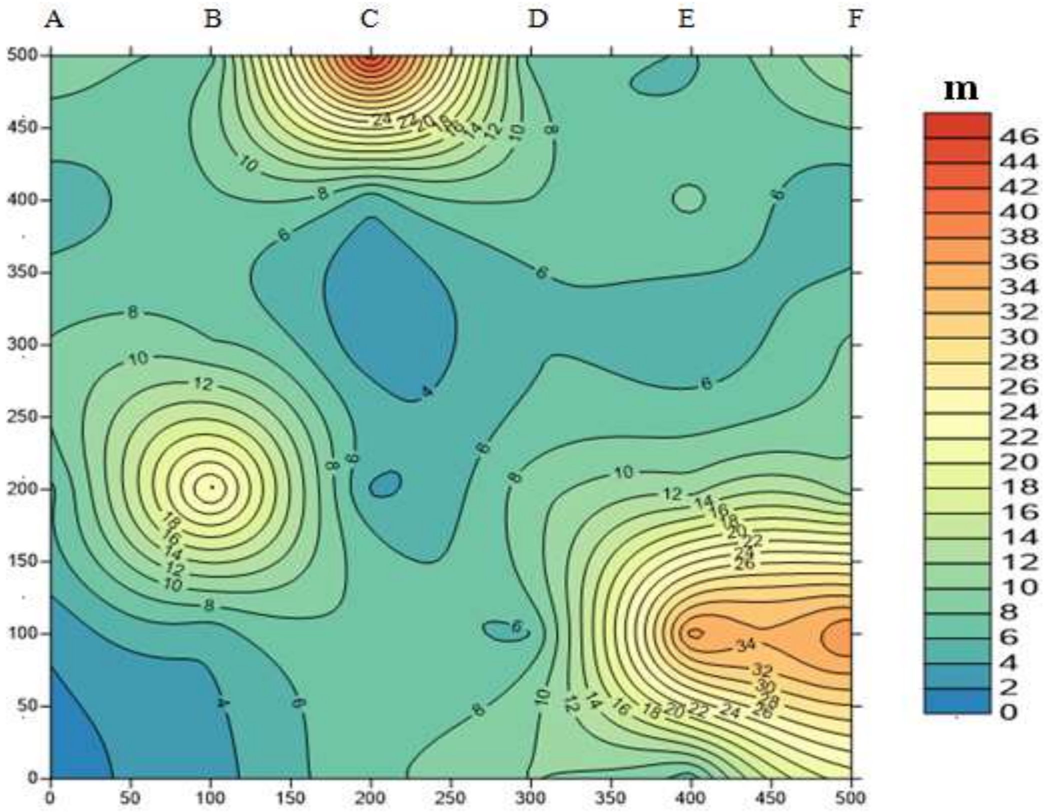

Fig. 10: Depth to consolidated rocks

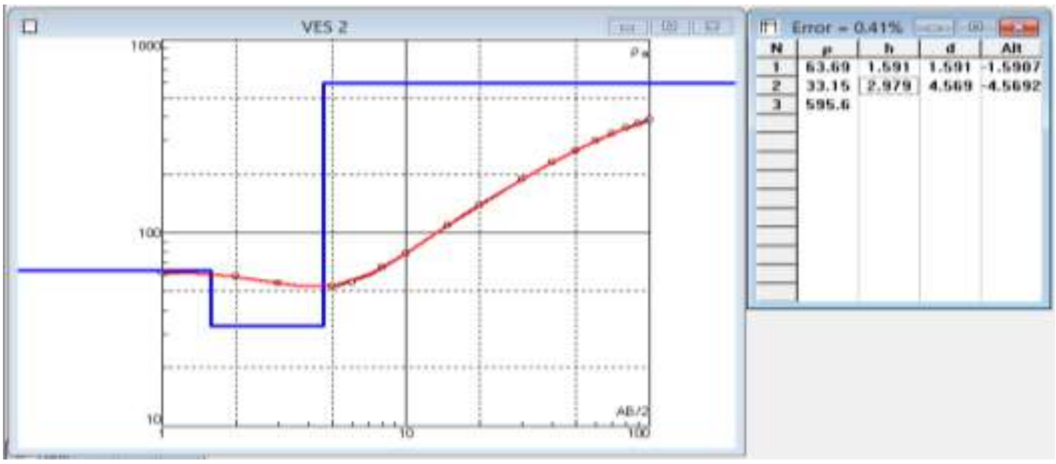

Fig. 11: Curve of VES 2 B2 on Profile B

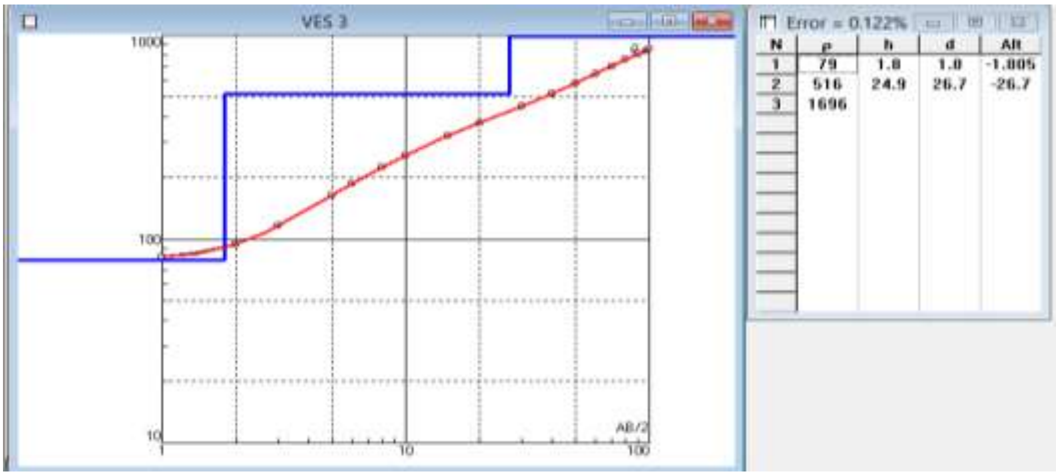

Fig. 12: Curve of VES 3 B3 on Profile B

Conclusions

The entire subsurface of the Proposed Stadium, is made up of three (3) distinctive layers; the Top Soil/Lateritic Particles with resistivity value of 20.38 to 272.8 Ω*m* it thickness ranges between 0.09 to 5.84 m, the Weathered Basement Rocks with resistivity value of 12.39 to 1566 Ω*m*, it thickness ranges between 0.49 to 44.62 m and the Fresh Basement rocks with resistivity of 595.6 to 3606 Ω*m* characterised this layer, it is deepest at the following VES point A6, B3, B4, C6, C1, C2, D1, D3, E2, E3, F2 and F1. It is also very shallow at the following VES points; A1, B1, C4, D4, E6 and F5. The depth to the basement rocks (Fig. 10) varied between 0.09 m A6 (VES 6) and 5.84 m E3 (VES 3).

Concerned Authority and Contractors who wish to construct the international stadium are encouraged to make use of the results of this study to reduce the problem of stadium building collapse and cracking of building walls and foundations. In view of the result obtained, Water boreholes can be drilled on the following VES points; A6, B3, B4, C6, C1, C2, D1, D3, E2, E3, F2 and F1, these VES points depicts zones of good fractures that can serve as source of groundwater. Finally, Geoelectrical investigation can help determined the depth to bedrocks in any construction site, with this, the cost that supposed to be required could be drastically reduced. It will thereby, save time and any other resources. Through this study, it was confirm that the Schlumberger electrical configuration or resistivity sounding method is an efficient tool for investigating the depth to consolidation in a basement environment.

Conflict of Interest

Authors declare that there is no conflict of interest reported in this work.

References

Aderoju A Ademola & Adebayo O Ojo 2015. Geophysical investigation for foundation studies at Ogudu River Valley Estate, Lagos, Southwestern, Nigeria. *The Pacific J. Sci. and Techn.*, 16(1): 295-304.

Alabi AA 2011. Geology and environmental impact assessment and benefit of granitic rocks of Minna Area, Northwestern Nigeria. *Ethiopian J. Envtal. Stud. and Mgt.*, 4(4): 39-44.

Alexey Bobachev 2003. IPI2WIN Resistivity Sounding Interpretation (Version 3.0.1.a 7.01.03). Mosco State University.

Bell FG 2007. Engineering Geology. Oxford, United Kingdom: Elsevier Ltd.

National Population Commission 2010. 2006 Population and Housing Census, Priority Table 3.

Qing-KeNie, Jian-peng Li, Hua-wei Li & Shu-qi Liang 2014. Distribution and forming mechanism of Karst Collapses in Tangshan Stadium. *J. Geotechn. and Geoenv. Engr.*, 3(1): 332-345.

Ranker, www.m.ranker.com/list of football stadium collapse.